First description and classification of the ozone hole over the Arctic in boreal spring 2020

Martin Dameris[1], Diego G. Loyola[2], Matthias Nützel[1], Melanie Coldewey-Egbers[2], Christophe Lerot[3], Fabian Romahn[2], Michel van Roozendael[3]

[1]Deutsches Zentrum für Luft- und Raumfahrt, Institut für Physik der Atmosphäre, Oberpfaffenhofen, Weßling, Germany.
[2]Deutsches Zentrum für Luft- und Raumfahrt, Institut für Methodik der Fernerkundung, Oberpfaffenhofen, Weßling, Germany.
[3]Royal Belgian Institute for Space Aeronomy, Uccle, Belgium.

Correspondence to: Martin Dameris (martin.dameris@dlr.de)

Abstract. Ozone data derived from the TROPOMI sensor onboard the Sentinel-5 Precursor satellite are showing an atypical ozone hole feature in the polar region of the Northern hemisphere (Arctic) in spring 2020. A persistent ozone hole pattern with minimum total ozone column values around or below 220 Dobson units (DU) was seen for the first time over the Arctic for about 5 weeks in March and early April 2020. Usually an ozone hole with such low total ozone column values has only been observed in the polar Southern hemisphere (Antarctic) in spring over the last 4 decades, but not over the Arctic. The ozone hole pattern was caused by a particularly stable polar vortex in the stratosphere, enabling a persistent cold stratosphere at higher latitudes, a prerequisite for ozone depletion through heterogeneous chemistry. Based on the ERA5 reanalysis from ECMWF, the Northern winter 2019/2020 (from December to March) showed minimum polar cap temperatures consistently below 195 K around 20 km altitude, which enabled enhanced formation of polar stratospheric clouds. The special situation in spring 2020 is compared and discussed in context with two other ozone hole-like features in spring 1997 and 2011 that were showing comparable dynamical conditions in the stratosphere in combination with low total ozone column values. However, during these years total ozone columns below 220 DU over larger areas and over several consecutive days have not been observed. The similarities and differences of the atmospheric conditions of these three events and possible explanations are presented and discussed. It becomes apparent that the monthly mean of the minimum total ozone column value for March 2020 (i.e. 221 DU) was clearly below the respective values found in March 1997 (i.e. 267 DU) and 2011 (i.e. 252 DU), which emphasizes the noteworthiness of the evolution of the polar stratospheric ozone layer in Northern hemisphere spring 2020. These results provide a first description and classification of the development of the Arctic ozone hole in boreal spring 2020 and highlight its peculiarity.

1 Introduction

Today's operating satellite instruments produce a reliable picture of the Earth's atmosphere and its chemical composition. These instruments monitor, for example, the evolution of the stratospheric ozone layer (e.g., Loyola et al., 2009), which is important for life on Earth. An ozone hole, a region with unusually low ozone values, can occur in polar regions if chemical and dynamical processes are interacting in a specific way that allow for strong ozone depletion and hamper meridional transport of ozone rich air from lower latitudes.

The largest concentrations of atmospheric ozone are found in the stratosphere, in the so-called ozone layer, with about 90% of ozone abundance being located at an altitude between 15 and 30 km (e.g., Langematz, 2019). The Dobson unit (DU) – named after Gordon Dobson (1889-1976), who devised the first instrument for measuring atmospheric ozone content – is used to describe the total amount of ozone found in the atmosphere above a specific location. Typically an ozone hole is defined as the area where the total ozone column (TOC) decreases to values of less than 220 DU. In the Southern hemisphere polar region (Antarctic) a TOC below 220 DU is about 30% under the expected ozone value in austral spring. Climatological mean TOCs averaged over the Northern polar region (Arctic) in boreal spring are higher (~400-450 DU; e.g., Dameris, 2010), and therefore the decrease of TOC below 220 DU during this period indicates a reduction in the order of 50%.

Due to the prohibition of the production and usage of ozone depleting substances (among others CFCs: chlorofluorocarbons) in response to the international activities to protect the ozone layer (Montreal Protocol: multilateral environmental agreement of the United Nations, signed in 1987, and its amendments) atmospheric concentrations of these chemical substances (particularly CFCs) and their products have been reduced over the last 20 years by about 15% (Chapter 1 in WMO, 2018). Nevertheless, the current atmospheric content of CFCs is still enhanced as CFCs have lifetimes of several decades (SPARC, 2013). Consequently, the chlorine concentration in the stratosphere is still high. Based on the current scientific understanding, the chlorine content is expected to reach pre-CFC-era conditions (i.e. levels similar to the ones before 1980) around the middle of this century, and therefore we can expect a full recovery of the ozone layer in the next 30 to 40 years (see Chapters 3 and 4 in WMO, 2018).

Notwithstanding the Montreal Protocol and the projected recovery of the ozone layer, very low temperatures in the polar lower stratosphere in any particular year, which are due to a strong and stable polar vortex in winter, can lead to heavy ozone depletion in early spring, not only in the Southern hemisphere, but also in the Northern hemisphere. Exemplarily, in March 2020 very low TOC values were measured in the Arctic although the stratospheric chlorine content in 2020 is known to be clearly lower than in previous years (Chapter 1 in WMO, 2018).

The dynamical conditions of the stratosphere as observed in Northern hemisphere spring 2020 were unusual, showing a stable polar stratospheric vortex with low temperatures. Two other extreme situations have been noted in the literature, indicating comparable dynamical conditions in the Northern stratosphere in spring: 1997 (e.g., Lefèvre et al., 1998; Hansen and Chipperfield, 1999) and 2011 (e.g., Manney et al., 2011). However TOC below 220 DU have not been observed in these

two years. Although the dynamical conditions this winter and spring 2019/2020 were unusual, atmospheric researchers have expected the possible occurrence of such conditions because they are in the natural range of stratospheric dynamical fluctuations in Northern winter and early spring. The importance of stratospheric dynamics with respect to low TOC has been discussed in detail in the last decades (e.g., Chapters 4 and 12 in WMO, 1999; Chapter 3 in WMO, 2003; Rex et al., 2004; Tilmes et al., 2006; Kivi et al., 2007; Harris et al., 2010; Chapter 3 in WMO, 2014).

Nevertheless, it was unexpected to detect such low TOC values – falling even below the typical ozone hole threshold of 220 DU, which was devised for the Southern hemisphere – in the polar stratosphere in Northern hemisphere spring in 2020 (Figure 1), despite the reduced chlorine content in the stratosphere. The occurrence of TOC values below 220 DU in March 2020 derived from satellite instrument measurements is confirmed by ground-based measurements at different Northern hemisphere stations, in particular at stations in Canada (for instance Alert, Eureka, and Resolute; current data are available at http://www.temis.nl/uvradiation/UVarchive/stations_uv.html; see van Geffen et al., 2017).

This study provides a descriptive presentation of the recent dynamical situation in northern winter and spring 2019/2020, which led for the first time to an ozone hole with TOC below 220 DU over the Arctic. It allows a classification of the current situation by the comparison of similar dynamical conditions in spring of other years, but which did not show such low TOC values below 220 DU over the polar Northern hemisphere in spring.

In the next Section (Sect. 2) the data sets used for our analyses are introduced including a short description of the performed data processing. In Section 3 the special situation in Northern hemisphere winter and spring 2019/2020 is presented in detail and in Section 4 it is compared with two Northern hemisphere winter and spring periods, namely 1996/1997 and 2010/2011, where similar polar stratospheric conditions – including low TOC values – have been observed. The discussion of results and the conclusions are presented in Section 5 and Section 6, respectively.

2 Data and data processing

Meteorological data

In this study the presented dynamical analyses are based on meteorological data derived from ECMWF's most recent atmospheric reanalysis, ERA5 (Hersbach et al., 2019, 2020). For our investigations the ERA5 data was downloaded at 0.25°x0.25° resolution. Daily mean data are prepared for the presentations of the respective meteorological situations. They are produced using hourly data on pressure levels (Copernicus Climate Change Service (C3S), 2018) and using the CDO (climate data operators; Schulzweida, 2019) command ("daymean") to produce daily means from the hourly data. Monthly mean values are obtained from the monthly mean data at pressure levels (Copernicus Climate Change Service (C3S), 2019). The focus is laid on stratospheric zonal winds and polar temperatures. ERA5 (raw) data is publicly available. For details see the data availability section.

Ozone data

Ozone data from July 2019 to April 2020 from the TROPOMI sensor onboard the EU/ESA Copernicus Sentinel-5 Precursor satellite are scientifically used for the first time in combination with the long-term ozone data set from the European satellite data record GOME-type Total Ozone Essential Climate Variable (GTO-ECV) from July 1995 to June 2019 (Coldewey-
5 Egbers et al., 2015). The publicly available (Level 2) TOC for July 2019 to April 2020 are derived from the TROPOMI sensor using the GODFIT algorithm (Lerot et al., 2014). The estimated mean bias of the TROPOMI total ozone compared with ground-based measurements is less than ±1 % with a mean standard deviation of up to ±1.6-2.5 % (Garane et al., 2019). The TROPOMI TOC images presented first in this study are based on daily mean data regridded to 1°x1° resolution to facilitate the comparison with the GTO-ECV data. For details see the data availability section.

10 GTO-ECV has been developed in the framework of the European Space Agency's Climate Change Initiative ozone project and is based on observations from the satellite sensors GOME/ERS-2, SCIAMACHY, OMI, and GOME-2 covering the time period from July 1995 to June 2019 (Coldewey-Egbers et al., 2015). The agreement between GTO-ECV and ground-based observations is 0.5%-1.5% peak-to-peak amplitude with a negligible long-term drift in the Northern hemisphere (Garane et al., 2018) and the difference between GTO-ECV and an "adjusted" TOC data set based on reanalysis data is between
15 −0.5±1.7 % and −1.0±1.1 % (for details see Coldewey-Egbers et al., 2020). In particular the excellent temporal stability makes the GTO-ECV data record suitable and useful for applications related to long-term investigations of the ozone layer. In this study we use the daily mean data product at 1°x1° resolution to analyse minimum ozone columns in the Northern hemisphere polar region during the past 24 years. It must be noted that during polar night the used satellite sensors cannot provide measurements. For instance in December, north of about 70°N no observations are available. With returning sunlight
20 the coverage in the northern high latitude regions improves and global coverage is resumed around March 20.

3 Situation in Northern winter and spring 2019/2020

In the Arctic winter and early spring 2019/2020 the stratospheric polar vortex turned out to be persistent with strong zonal winds from mid-December until early April. Our analysis of ERA5 data at 60°N, 10 hPa (about 30 km altitude) shows strong zonal mean zonal wind speeds (magenta line and dots in Figure 2), which are high with respect to the monthly mean values
25 for the time period from 1979/1980 to 2019/2020 (see grey dots in the figure). There were some smaller dynamical fluctuations in winter 2019/2020, which were caused by planetary wave activity (which is also indicated by variations of meridional heat and momentum fluxes at mid-latitudes, 100 hPa (Newman et al., 2001); not shown here; but see https://acd-ext.gsfc.nasa.gov/Data_services/met/ann_data.html or https://ozonewatch.gsfc.nasa.gov/). No specific warmings of the polar stratosphere were observed (see below) and the shape of the vortex and its position was not severely deteriorated, except for
30 the period from mid-January to beginning of February 2020, as hinted in Figure 2. The ERA5 monthly mean zonal winds

derived for the Northern hemisphere in January, February and March in 2020 are clearly indicating a persistent strong polar vortex, with maximum zonal wind speeds at 10 hPa of up to 118 m/s in January (Figure 3).

These dynamical conditions in winter 2019/2020 allowed a strong cooling of the lower stratosphere in the inner part of the polar vortex during polar night, especially in January, February and March (Figure 4). The monthly mean temperatures in the

5   lower stratosphere (at 50 hPa, about 20 km altitude) in January, February and March were very low in comparison with the respective mean values calculated for the last 4 decades (1979/1980-2019/2020). In March 2020 the calculated maximum temperature difference with respect to the long-term mean was −23.8 K. Minimum polar temperatures below 195 K at 50 hPa (i.e. the Cl activation threshold at this altitude, see for instance Figure 4-1 of Chapter 4 in WMO, 2018) were detected in the polar cap region (50°-90°N) from the beginning of December until end of March (magenta line in Figure 5). Further

10   analyses of the temperature field at 50 hPa indicate large areas below 195 K (magenta line in Figure 6). The maximum daily mean area of temperatures below 195 K is $13 \cdot 10^{12}$ m^2, which is found end of January. At the end of March the daily cumulative area below 195 K results to about $920 \cdot 10^{12}$ m^2. This led to conditions allowing the formation of polar stratospheric clouds (PSC) of type I (Nitric Acid Trihydrate (NAT) particles), for about 3.5 months. When the sun rises in spring, sunlight delivers the energy required for starting a chemical depletion process of ozone (e.g., Dameris, 2010).

15   Stratospheric ozone can then be destroyed by heterogeneous chemical reactions due to the still enhanced atmospheric chlorine content (caused by CFC emissions in last decades). As a consequence, in spring 2020 an Arctic ozone hole, i.e. a region with TOC values below 220 DU, has developed within the boundaries of the stable polar vortex for eight continuous days from March 12 to 19 (Figure 1; see also the magenta line in Figure 7). A region of significantly reduced total ozone column values, i.e. an ozone hole-like pattern, was observed over the polar cap from the beginning of March until early April

20   2020 (Figure 1).

The temporal evolution of minimum TROPOMI TOC values north of 50°N from July 2019 until April 2020 is presented in Figure 7 (magenta line) and compared with historical values from the GOME-type Total Ozone Essential Climate Variable (GTO-ECV) data record (see Section 2 for details). In winter 2019/2020 ozone values were most of the time slightly below mean conditions until the end of February with respect to mean minimum TOC values (Figure 7, magenta line vs. thick black

25   line). But there were several short-term deviations towards even lower TOC, during so-called ozone mini-hole events. The most noteworthy examples occurred in early December 2019 (Dec 3 and Dec 4), beginning of January 2020 (Jan 4 and Jan 5, and Jan 7 and Jan 8), and the end of January (Jan 25 to Jan 27). Ozone mini-holes are synoptic-scale features (with a high pressure system in the troposphere below the stratospheric polar vortex, i.e. a low pressure area) with significantly reduced TOC values, which are – to large parts – unrelated to (heterogeneous) chemical processes. It is well understood that ozone

30   mini-holes are primarily resulting from dynamical processes (e.g., Millán and Manney, 2017). The positions of the mini-holes correlate well with minima of potential vorticity near the tropopause (Peters et al., 1995; James and Peters, 2002). Hoinka et al. (1996) found that about 50% of short-term TOC fluctuations in the Northern hemisphere can be explained by variations of the tropopause pressure. Furthermore, Steinbrecht et al. (1998) showed that an increase of tropopause height by

one kilometer is connected with a reduction of TOC by 16 DU. Figure 7 illustrates that such mini-hole events occur regularly (the lower light grey line) during Northern winter. Very commonly the ozone mini-holes are created in the Northern Atlantic region and then they often drift eastward towards Northern Europe within a few days (James, 1998). This was also the case for the three examples seen in winter 2019/2020 with minimum TOC found over Northern Europe (not shown). Since the polar vortex existed already in late November and early December 2019 with lower than usual TOC, for instance the ozone mini-hole on December 3 and 4 showed very low TOC values (170 DU; Figure 7) at 65°N, north-east of UK and west of Scandinavia.

As the polar vortex was stable and strong since the beginning of the winter 2019/2020, an ozone hole-like pattern is expected from January 2020 onwards, but with TOC values above 220 DU inside the vortex. The stable polar vortex with strong zonal winds should have prevented the meridional transport of ozone rich air from lower latitudes towards the Northern polar region. This is for instance indicated by ground-based measurements at different Northern hemisphere stations (data are available at http://www.temis.nl/uvradiation/UVarchive/stations_uv.html; see van Geffen et al., 2017) with lower TOC values in the inner part of the polar vortex and higher TOC values outside. After mid-February the ozone hole-like feature can be identified also in the TROPOMI TOC values, which is indicated by a strong horizontal gradient in the vicinity of the polar jet with strongest zonal winds.

Outstanding deviations from normal conditions could be found starting in early March 2020 until early April, when low TOC values in the North polar region were detected (Figure 7): the long period of unusual low TOC started in early March 2020, falling below 220 DU for the first time on March 2, and continued with similar low TOC – including a period of 8 consecutive days with minimum TOCs below 220 DU – until April 7. For the first time TOC values near or below 220 DU were observed for a period of about 5 weeks corresponding to new record low values for this time of the year. The maximum ozone hole area (with TOC below 220 DU) was determined with 0.9 million km^2 (= 0.9·10^{12} m^2), which was detected on March 12 (Figure 1). The daily accumulated ozone hole area in March and April was estimated with 4 million km^2.

4 Situations in Northern winter and spring 1996/1997 and 2010/2011

There are two other prominent late winter / early spring periods in the Northern hemisphere, which showed similar stable and cold stratospheric polar vortices. In particular, comparable dynamical conditions in the Northern stratosphere were observed in February and March 1997 (e.g., Lefèvre et al., 1998; Hansen and Chipperfield, 1999) and 2011 (e.g., Manney et al., 2011).

In Figure 2 the temporal evolution of the two polar vortices in 1996/1997 (blue line) and 2010/2011 (green line) is indicated by the zonal mean zonal wind speed at 60°N, 10 hPa. In comparison with the dynamical situation in January, February and March 2020 (magenta line in Figure 2), the respective time periods in 1997 and 2011 showed also a persistent polar vortex with high zonal wind speeds, which reached values of up to more than 50 ms^{-1}. These values are higher than the long-term

mean values, which show an increase up to 40 ms^{-1} until the beginning of January and a decrease afterward (see also Figure 1 in Lee and Butler, 2020). While the temporal evolution of the dynamical situation in spring 2011 was very similar to the one in 2020 with a persistent polar vortex and high zonal wind speeds until mid-March, the period of strong zonal winds in 1997 continued until April. The polar vortex in December 1996 was weak and therefore polar temperatures were relatively

5   high (higher than 195 K; see below). The evolution of the winter vortices in December 2010 and 2019 are similar reaching zonal wind speeds of about 40 ms^{-1} in mid-December.

In all three years the respective February and March dynamical conditions led to similar significant cooling of the polar cap (50°N-90°N) in early spring. In Figure 5 the temporal evolution (based on daily values) of the detected minimum temperatures at 50 hPa is shown. In February and March the minimum temperatures were below 195 K in all three years, the

10   threshold temperature value for the formation of polar stratospheric clouds (NAT-PSC). The determined minimum temperatures in December 2019 and January 2020 were mostly lower at 50 hPa compared to the minimum temperature values detected in December/January 1996/1997 and December/January 2010/2011. The minimum values of the monthly mean temperatures are given in Table 1, indicating the characteristic of low temperatures in December 2019 and January and February 2020 (see also the colored dots in Figure 5).

Table 1: Minimum temperatures (in Kelvin) of the polar cap region (50°N-90°N) at 50 hPa (about 20 km altitude) based on the monthly mean temperatures from ERA5 in December, January, February and March of 1996/1997, 2010/2011, 2019/2020 and the long-term mean values (1979/1980-2019/2020), respectively.

Min. temp. 50 hPa	December	January	February	March
1996/1997	201.3	196.5	191.8	192.7
2010/2011	195.6	194.2	191.2	194.7
2019/2020	194.3	190.7	190.8	194.6
Long-term means (1979/1980-2019/2020)	197.0	195.6	199.5	205.5

As demonstrated in Figure 6, the daily areas with temperatures below 195 K at the 50 hPa pressure level are obviously larger in 2019/2020 (magenta line) than in 1996/1997 (blue line) and 2010/2011 (green line). In particular, the cumulated areas are markedly different: whereas in 2019/2020 the cumulated area was about $920 \cdot 10^{12}$ m^2, in 1996/1997 it was about $370 \cdot 10^{12}$ m^2

25   and in 2010/2011 it was about $650 \cdot 10^{12}$ m^2. Furthermore, in the last week of January 2020 the temperatures at 50 hPa went

below 188 K (magenta line in Figure 5), the typical ICE-PSC threshold (PSC type 2; see for instance Figure 4-1 of Chapter 4 in WMO, 2018). The maximum daily area was determined with $2.8 \cdot 10^{12}$ m^2 on January 30, and the cumulated area reached its maximum of $18 \cdot 10^{12}$ m^2 on March 2, 2020. While the threshold for ICE-PSC was not reached in 1996/1997, in 2010/2011 the cumulated area with temperatures below 188 K was estimated with $4.3 \cdot 10^{12}$ m^2.

5 To summarize, in all three years the temperatures in the lower stratosphere in February and March were in a similar temperature range, showing colder conditions than usual. In addition, December 2019 and January 2020 were also colder than the long-term mean conditions (Table 1). The minimum temperatures in the lower stratosphere in December/January 2019/2020 were lower than in December/January 1996/1997 and 2010/2011. Therefore, the thermal conditions in winter 2019/2020 were enabling enhanced formation of larger PSC fields, starting from the beginning of the winter until early

10 spring. Having permanent presence of polar stratospheric clouds over about four months enabled more efficient chlorine activation. In addition, they should have supported strong denitrification of the lower stratosphere by irreversible removal of total reactive nitrogen (NO$_y$), especially HNO$_3$, due to heterogeneous reaction on the surface of PSCs followed by sedimentation of PSC particles (Fahey et al., 1990). This ultimately enabled a longer than usual period of chemical ozone depletion (e.g., Fahey et al., 1990; Rex et al., 1999, Pommereau et al., 2018). The occurrence of denitrification is very likely

15 for the winter 2019/2020, but so far we cannot present a definite analysis for this hypothesis.

The temporal evolution of minimum TOC values north of 50°N between July 1996 and June 1997 (blue line in Figure 7) and between July 2010 and June 2011 (green line in Figure 7) indicates normal or slightly enhanced ozone values until February with respect to the long-term mean value (thick black line), which is based on satellite observations from 1995 to 2019. In February 1997 and February 2011, TOC maps from the Northern polar region were both showing typical features of a

20 stronger polar vortex with lower TOC values within the vortex and relatively high TOC values in the collar region of the polar vortex (not shown). Around the beginning of March 1997 and March 2011 the TOC values were declining and low TOC values were detected in both years until early April. Figure 8 is showing the TOC monthly means for March 1997, 2011, and 2020. Three ozone hole-like patterns with low TCO values over the polar cap can be seen. The lowest TOC values are clearly detected in boreal spring 2020. In spring 1997 and 2011 TOC values below 220 DU were not detected over larger

25 areas and over several consecutive days. The monthly mean minimum TOC value for March 2020, which is 221 DU, is much lower compared to the monthly mean minimum TOCs for March 1997 (267 DU) and for March 2011 (252 DU).

5 Discussions

The Arctic winter and early spring total column ozone variability in the recent decades is in large parts reflecting the natural fluctuations of the stratospheric dynamics of the Northern hemisphere during this period (Chapter 4 in WMO, 2018). The

30 same can be stated about the Southern hemisphere, where in most cases the interannual fluctuations of the strength of the Antarctic ozone hole can be explained by different dynamical conditions of the stratosphere (e.g., Chapter 4 in WMO, 2018).

Dynamical conditions of the Northern stratosphere at higher latitudes in winter can range from a very disturbed polar vortex (i.e. by strong planetary wave activity), which leads to high stratospheric temperatures, to conditions with a persistent stable polar vortex (i.e. with low planetary wave activity), which creates low stratospheric temperatures.

Therefore, on the one hand, it is possible to find extreme situations with strong mixing of air masses in the polar regions (for instance during major stratospheric warmings) in combination with reduced chemically induced ozone depletion, which leads to enhanced TOC values. On the other hand, situations with significantly suppressed meridional air mass exchange and transport into the polar vortex area can be found in combination with enhanced ozone depletion by heterogeneous chemical processes inside the vortex, which causes a clear reduction of TOC. The latter was the case in winter and spring 2019/2020. Our comparative analysis of 2019/2020 with respect to the last four decades (i.e. the length of the ERA5 data set) indicates an extra-ordinary dynamical situation with a persistent strong and cold polar vortex over the complete season. There is further evidence that a similar dynamical event did not happen in the period from 1955 to 1980, i.e. before the starting point of our dynamical analyses based on ERA5. A look into the historical data set, which was provided by the Stratospheric Research Group at FU Berlin (e.g., Labitzke and Naujokat, 2000), indicates that the winter and spring 1996/1997 was the coldest within the Berlin time series ranging from 1955 to 2000. In combination with our research results this suggests that the dynamical situation of the winter and spring 2019/2020 is outstanding since the beginning of monitoring the stratosphere in the 1950s.

We recall that the stratospheric dynamical conditions were completely different in the Northern winter 2018/2019 (brown line in Figure 2) compared to 2019/2020 (magenta line in Figure 2) showing a sudden major stratospheric warming event, which started in late December 2018. In the first half of January 2019 the direction of the mean zonal wind (60°N, 10 hPa) changed its direction from westerlies to easterlies. This strong disturbance of the polar vortex by planetary waves led to a pronounced warming of the lower stratosphere (e.g., Lee and Butler, 2020), indicating minimum temperatures in the polar cap region, which were clearly above the threshold for the formation of NAT-PSC (195 K) for the complete winter season including early spring (brown line in Figure 5). Consequently, comparatively high TOC values (around the long-term mean) in the Arctic region were found from late winter to early spring (not shown).

Another example of the importance of stratospheric dynamics regarding the development of low TOC values was the evolution of the ozone values in Southern hemisphere spring 2019 (not shown). A strong polar stratospheric warming (about 50 K at 80°S, 30 hPa within several days) happened over the Antarctic in the beginning of September 2019 (e.g., Lim et al., 2020). Afterwards the stratospheric polar vortex was weak leading to much warmer conditions in the polar region, with unusual high stratospheric temperatures for this time of the year. After mid-September minimum polar cap temperatures at 50 hPa were consistently higher than 195 K. The TOC values in the Antarctic were noticeably higher in 2019 than in previous years (not shown; see for instance https://public.wmo.int/en/media/news/antarctic-ozone-hole-smallest-record; October 24, 2019).

The Arctic observations in 2020 are consistent with our expectation that Arctic ozone losses in spring are largest after cold stratospheric winters (Chapter 4 in WMO, 2018). If the dynamical conditions in the Northern hemisphere winter and early spring season (January, February, March) are similar to the conditions found during Southern hemisphere winter to spring (August, September, October) with a persistent stable and cold polar vortex, the ozone depletion rates are comparably strong

5 as a result. Therefore, it is obvious that the dynamical conditions of the stratosphere are triggering the occurrence of heterogeneous ozone depletion and therefore the formation of an ozone hole.

The dynamical conditions in the Arctic stratosphere in February and March 2020 were similar to the other two exceptional stratospheric dynamics situations in early spring 1997 and 2011. Consequently, all three years showed particularly strong ozone depletion with low TOCs in March (Figure 7). Noteworthy about March 2020 is that minimum TOC values were

10 below 220 DU for several days, although the stratospheric chlorine content was lower than in 1997 and 2011. Our comparisons show that especially in December 2019 and January 2020 the temperatures in the lower stratosphere were lower than in the two other years discussed here. In 2019/2020 the minimum polar cap temperatures at 50 hPa were all the time below 195 K (the threshold for formation of NAT-PSC) in December, January, February and most of March. Our analyses show that the daily areas allowing for the formation of PSC were clearly larger in 2019/2020 in comparison to the winters

15 1996/1997 and 2010/2011. The ERA5 data set also indicates minimum temperature values in winter 2019/2020, which were slightly above or below 188 K for a week (in particular at the end of January 2020), providing conditions for the formation of ICE-PSCs.

Since the polar vortex in winter and spring 2019/2020 provided continuous conditions for the formation of PSCs, significant denitrification of the stratosphere should have occurred, i.e., a permanent removal of total reactive nitrogen (NO_y, primarily

20 HNO_3) by the sedimentation of NAT-PSC particles (Fahey et al., 1990) is expected. In this case, this would have contributed to the five week period of significant TOC reduction by an extended phase of active stratospheric chlorine. As said, so far we cannot underline our suspicion by definite analyses. However, the observed minimum TOC values in March 2020 with new low TOC records for the Northern hemisphere polar cap were pointing to substantial ozone depletion, although the background chlorine content in 2020 was lower than in the years 1997 and 2011. Here we note that 2020 was also starting at

25 lower base values of TOC (inside the polar vortex; see Figure 7). This will also contribute to the fact that the spring TOC values in the Arctic region in 2020 were clearly lower than those found in 1997 and 2011.

From our current point of view, the situation with an atypical ozone hole over the Arctic in 2020 is not an unequivocal result of climate change. The dynamical situations in February and March of 1997 and 2011 in comparison to 2020 were similar. Beyond that the cold stratosphere in December 2019 and January 2020 as a single event does not point towards climate

30 change due to increasing greenhouse gas concentrations. From our point of view, the Northern hemisphere winter 2019/2020 is a perfect showcase that a Northern winter with less planetary wave activity, and therefore a strong and stable vortex with low temperatures is possible. Only if similar conditions would happen more regularly in the next years, then this could be a sign of climate change. Although the stratosphere is more or less cooling steadily due to increasing greenhouse gas

concentrations (Maycock et al., 2018), consequences for stratospheric dynamics particularly in winter and ozone depletion in spring are still under debate (e.g., Pommereau et al., 2018). For instance the empirical quantification of the relation between winter-spring loss of Arctic ozone and changes in stratospheric climate by Rex et al. (2004) showed the possibility that cold (northern) winters are getting colder in future. It is possible that the cooling of the (lower) stratosphere could delay the

5 recovery of the ozone layer (Pommereau et al., 2018). But this statement is in contradiction with results derived from Chemistry-Climate model predictions (e.g., Langematz et al., 2014; Dhomse et al., 2018) indicating that climate change in the Northern hemisphere will accelerate stratospheric ozone recovery instead of delaying it (see also Chapters 3 and 4 in WMO, 2018). On the other hand, more than 20 years ago model calculations by Waibel et al. (1999) showed that higher degrees of Arctic denitrification in future, related to stratospheric cooling by enhanced greenhouse gas concentrations, could

10 lead to larger seasonal ozone depletion despite the projected decline in inorganic chlorine.

Finally, based on our current knowledge we deem it unlikely that the observed enhanced CFC-11 emissions in recent years (Montzka et al., 2018) have significantly influenced the ozone depletion in the Northern hemisphere in 2020 (Dameris et al., 2019; Fleming et al., 2020; Keeble et al., 2020). The impact of the additional CFC-11 emissions should be of minor importance.

15 **6 Conclusions**

This study aims to present in a first step a consistent description of the Northern winter and spring season 2019/2020 regarding the dynamical situation of the stratosphere and the evolution of the ozone layer in the Arctic region. For the first time an Arctic ozone hole is detected, meaning that TOC values were in the vicinity or below 220 DU over a larger area (up to 0.9 million km^2) and for a longer time period (about a five weeks). The 2019/2020 situation is confronted with other years,

20 which are showing similar stratospheric dynamics in spring. We have used most recently available data sets for the preparation of presented analyses, (i) meteorological data from ERA5 and (ii) total ozone column data sets, i.e. GTO-ECV (based on the European satellite sensors GOME/ERS-2, SCIAMACHY, OMI, and GOME-2) in combination with TROPOMI onboard Sentinel 5P. Although the detected Arctic ozone hole is much smaller in comparison to a typical Antarctic ozone hole – which is in the order of about 20 to 25 million km^2 (from early September until mid-October) and

25 TOC values below 220 DU are seen for up to about four months (WMO, 2018) – it is an extra-ordinary event because an ozone hole feature with TOC below 220 DU was not observed before. The results of our study pointed out that the persistent strong polar vortex in 2019/2020 (from mid-December to early April) led to particularly cold stratospheric conditions for the complete winter and early spring season, supporting the process of ozone depletion through heterogeneous chemistry. We have demonstrated that the special dynamical situation in winter 2019/2020 is relevant for this significant reduction of the

30 TOC in spring 2020, which occurred despite decrease in the stratospheric chlorine content over the last 2 decades.

If the regulations of the Montreal Protocol regarding the prohibition of CFCs are implemented strictly one can expect a full recovery of the ozone layer including the polar regions by the middle of this century (Chapters 3 and 4 in WMO, 2018). In recent years, the beginning of ozone recovery was already detected (e.g., Solomon et al., 2016; Weber et al., 2018). However, in the upcoming decades ozone holes will still occur in the Southern hemisphere, but also in the Northern

5 hemisphere under appropriate dynamical conditions with a stable polar vortex yielding a strong cooling of the polar lower stratosphere. Monitoring of the Earth's atmosphere from space is still an important task. The recovery of the ozone layer and its interactions with climate change must be carefully documented, as discussed for instance by Dameris and Loyola (2011). The data available from the different monitoring instruments enable well founded scientific explanations of special ozone features. For instance it is possible to explain the recent evolution of the ozone layer, in particular the occurrence of the

10 Arctic ozone hole in spring 2020 with new record low total ozone values for this region and period. This capability is crucial to allow a classification of specific events in the light of the Montreal Protocol.

Data availability. Meteorological data is based on ERA5 from ECMWF

15 (https://cds.climate.copernicus.eu/#!/search?text=ERA5&type=dataset), which is available at the Climate Data Store (CDS). This work contains modified Copernicus Climate Change Service information (2017, 2018, 2019). Neither the European Commission nor ECMWF is responsible for any use that may be made of the Copernicus information or data it contains. In particular, subsets, i.e. wind and temperature data, from the pressure level data sets of monthly averaged data (Copernicus Climate Change Service (C3S), 2019) and hourly reanalysis data (Copernicus Climate Change Service (C3S), 2018) have

20 been used. We thank the ECMWF for producing ERA5 data and making it available through the CDS. The used data contains modified Copernicus Climate Change Service information, in particular with respect to Figures 2, 3, 4, and 5 and Table 1. Please note, that the data used here may also contain "preliminary" ERA-5 data (cf. Hersbach et al., 2020).

The GTO-ECV Climate Research Data Package (ESA CCI, 2020) is available at http://cci.esa.int/ozone/ (last access: April 6, 2020), detailed information about this data record can be found at https://atmos.eoc.dlr.de/gto-ecv (last access: April 6,

25 2020). This data source is used here, in particular with respect to the preparation of Figures 7 and 8.

The (Level 2) TROPOMI total ozone column data (TROPOMI OFFL TOC; Copernicus Sentinel-5P, 2018) are available at https://s5phub.copernicus.eu/ (last access: May 18, 2020) and https://s5pexp.copernicus.eu/ (last access: May 18, 2020). This paper contains modified Copernicus Sentinel-5 Precursor data processed by DLR/BIRA/ESA. This data is used here, in particular with respect to Figures 1, 7, and 8.

30

Author contributions. MD structured and composed the paper. MD, DGL, MCE and MN jointly analyzed the different data sets and compiled the results including the preparation of the figures. MD, DGL, MCE and MN contributed to the writing of the manuscript. MCE, DGL, CL, and MvR generated the GTO-ECV data in the ESA project Ozone_cci+ and the EU/ECMWF project C3S_312b. CL, FR, DGL and MvR are responsible for the TROPOMI TOC Level 2 data in the ESA project S5P-MPC.

Competing interests. The authors declare that they have no conflict of interest.

Acknowledgements. First we would like to thank Birgit Hassler for an internal review of the first draft of the manuscript. The work for this study was supported under the umbrella of the DLR-project MABAK (Innovative Methoden zur Analyse und Bewertung von Veränderungen der Atmosphäre und des Klimasystems). The work described in this paper has also received funding from the ESA-projects "Ozone_cci" and "Ozone_cci+" (as part of the ESA Climate Change Initiative (CCI) program) and the Initiative and Networking Fund of the Helmholtz Association through the "Advanced Earth System Modelling Capacity (ESM)" project. The NCAR Command Language (NCL, 2018) was used for data analysis and to create some of the figures in this study. NCL is developed by UCAR/NCAR/CISL/TDD and is available online at https://doi.org/10.5065/D6WD3XH5. CDO (climate data operators; Schulzweida, 2019) was employed for processing the data.

References

Coldewey-Egbers, M., Loyola, D. G., Koukouli, M.-E., Balis, D., Lambert, J.-C., Verhoelst, T., Granville, J., van Roozendael, M., Lerot, C., Spurr, R., Frith, S. M., and Zehner, C.: The GOME-type Total Ozone Essential Climate Variable (GTO-ECV) data record from the ESA Climate Change Initiative, Atmos. Meas. Tech., 8, 3923–3940, https://doi.org/10.5194/amt-8-3923-2015, 2015.

Coldewey-Egbers, M., Loyola, D. G., Labow, G., and Frith, S. M.: Comparison of GTO-ECV and adjusted MERRA-2 total ozone columns from the last 2 decades and assessment of interannual variability, Atmos. Meas. Tech., 13, 1633-1654, https://doi.org/10.5194/amt-13-1633-2020, 2020.

Copernicus Climate Change Service (C3S), ERA5: Fifth generation of ECMWF atmospheric reanalyses of the global climate, Copernicus Climate Change Service Climate Data Store (CDS), *date of access May 11, 2020,* https://cds.climate.copernicus.eu/cdsapp#!/home, 2017.

Copernicus Climate Change Service (C3S), ERA5 hourly data on pressure levels from 1979 to present, Copernicus Climate Change Service Climate Data Store (CDS), https://cds.climate.copernicus.eu/cdsapp#!/dataset/10.24381/cds.bd0915c6, doi: 10.24381/cds.bd0915c6, 2018.

Copernicus Sentinel-5P (processed by ESA), TROPOMI Level 2 Ozone Total Column products, Version 01, European Space Agency, https://doi.org/10.5270/S5P-fqouvyz, 2018.

Copernicus Climate Change Service (C3S), ERA5 monthly averaged data on pressure levels from 1979 to present, Copernicus Climate Change Service Climate Data Store (CDS), https://cds.climate.copernicus.eu/cdsapp#!/dataset/10.24381/cds.6860a573, doi: 10.24381/cds.6860a573, 2019.

Dameris, M.: Climate change and atmospheric chemistry: How will the stratospheric ozone layer develop?, Angew. Chem. Int. Ed., 49, 8092-8102, doi: 10.1002/anie.201001643, 2010.

Dameris M., and Loyola, D. G.: "Chemistry-Climate Connections – Interaction of Physical, Dynamical, and Chemical Processes in Earth Atmosphere", in Climate Change - Geophysical Foundations and Ecological Effects, J. Blanco, H. Kheradmand (Eds), InTech, ISBN 978-953-307-419-1, pp. 1-26, 2011.

Dameris, M., Jöckel, P., Nützel, M.: Possible implications of enhanced chlorofluorocarbon-11 concentrations on ozone, Atmos. Chem. Phys., 19, 13759–13771, https://doi.org/10.5194/acp-19-13759-2019, 2019.

Dhomse, S., Kinnison, D., Chipperfield, M. P., Cionni, I., Hegglin, M., Abraham, N. L., Akiyoshi, H., Archibald, A. T., Bednarz, E. M., Bekki, S., Braesicke, P., Butchart, N., Dameris, M., Deushi, M., Frith, S., Hardiman, S. C., Hassler, B., Horowitz, L. W., Hu, R.-M., Jöckel, P., Josse, B., Kirner, O., Kremser, S., Langematz, U., Lewis, J., Marchand, M., Lin, V., Mancini, E., Marécal, V., Michou, M., Morgenstern, O., O'Connor, F. M., Oman, L., Pitari, G., Plummer, D. A., Pyle, J. A., Revell, L. E., Rozanov, E., Schofield, R., Stenke, A., Stone, K., Sudo, K., Tilmes, S., Visioni, D., Yamashita, Y., Zeng, G.: Estimates of ozone return dates from Chemistry-Climate Model Initiative simulations, Atmos. Chem. Phys., 18, 8409-8438, https://doi.org/10.5194/acp-18-8409-2018, 2018.

Fahey, D. W., Solomon, S., Kawa, S. R., Loewenstein, M., Podolske, J. R., Strahan S. E., and Chan, K. R.: A diagnostic for denitrification in the winter polar stratospheres, Nature, 345, 698-702, 1990.

Fleming, E. L., Newman, P. A., Liang, Q., and Daniel, J. S.: The impact of continuing CFC-11 emissions on stratospheric ozone, J. Geophys. Res., 125, e2019JD031849. doi.org:10.1029/2019JD031849, 2020.

Garane, K., Lerot, C., Coldewey-Egbers, M., Verhoelst, T., Koukouli, M.-E., Zyrichidou, I., Balis, D. S., Danckaert, T., Goutail, F., Granville, J., Hubert, D., Keppens, A., Lambert, J.-C., Loyola, D. G., Pommereau, J.-P., van Roozendael, M., and Zehner, C.: Quality assessment of the Ozone_cci Climate Research Data Package (release 2017) – Part 1: Ground-based validation of total ozone column data products, Atmos. Meas. Tech., 11, 1385–1402, https://doi.org/10.5194/amt-11-1385-2018, 2018.

Garane, K., Koukouli, M.-E., Verhoelst, T., Lerot, C., Heue, K.-P., Fioletov, V., Balis, D., Bais, A., Bazureau, A., Dehn, A., Goutail, F., Granville, J., Griffin, D., Hubert, D., Keppens, A., Lambert, J.-C., Loyola, D. G., McLinden, C., Pazmino, A., Pommereau, J.-P., Redondas, A., Romahn, F., Valks, P., van Roozendael, M., Xu, J., Zehner, C., Zerefos, C., and Zimmer,

W.: TROPOMI/S5P total ozone column data: global ground-based validation and consistency with other satellite missions, Atmos. Meas. Tech., 12, 5263–5287, https://doi.org/10.5194/amt-12-5263-2019, 2019.

Hansen, G., and Chipperfield, M. P.: Ozone depletion at the edge of the Arctic polar vortex 1996/1997, J. Geophys. Res., 104, 1837-1845, 1999.

5 Hersbach, H., Bell, B., Berrisford, P., Horányi, A., Sabater, J. M., Nicolas, J., Radu, R., Schepers, D., Simmons, A., Soci, C., and Dee, D.: Global reanalysis: goodbye ERA-Interim, hello ERA5, ECMWF Newsletter, 159, 17-24, https://doi.org/10.21957/vf291hehd7, 2019.

Hersbach, H., Bell, B., Berrisford, P., Hirahara, S., Horányi, A., Muñoz-Sabater, J., Nicolas, J., Peubey, C., Radu, R., Schepers, D., Simmons, A., Soci, C., Abdalla, S., Abellan, X., Balsamo, G., Bechtold, P., Biavati, G., Bidlot, J., Bonavita,
10 M., De Chiara, G., Dahlgren, P., Dee, D., Diamantakis, M., Dragani, R., Flemming, J., Forbes, R., Fuentes, M., Geer, A., Haimberger, L., Healy, S., Hogan, R.J., Hólm, E., Janisková, M., Keeley, S., Laloyaux, P., Lopez, P., Lupu, C., Radnoti, G., de Rosnay, P., Rozum, I., Vamborg, F., Villaume, S. and Thépaut, J.-N.: The ERA5 Global Reanalysis, Q. J. R. Meteorol. Soc., manuscript version of record online: 15 June 2020, doi: 10.1002/qj.3803, 2020.

Harris, N. R. P., Lehmann, R., Rex, M., and von der Gathen, P.: A closer look at Arctic ozone loss and polar stratospheric
15 clouds, Atmos. Chem. Phys., 10, 8499-8510, doi:10.5194/acp-10-8499-2010, 2010.

Hoinka, K. P., Claude, H., and Köhler, U.: On the correlation between tropopause pressure and ozone above central Europe, Geophys. Res. Lett., 23, 1753-1756, 1996.

James, P. M.: A climatology of ozone mini-holes over the northern hemisphere, Int. J. Climatol., 18, 1287-1303, https://doi.org/10.1002/(SICI)1097-0088(1998100)18:12<1287::AID-JOC315>3.0.CO;2-4, 1998.

20 James, P. M., and Peters, D.: The Lagrangian structure of ozone mini-holes and potential vorticity anomalies in the Northern Hemisphere, Ann. Geophys., 20, 835-846, https://doi.org/10.5194/angeo-20-835-2002, 2002.

Keeble, J., Abraham, N. L., Archibald, A. T., Chipperfield, M. P., Dhomse, S., Griffiths, P. T., and Pyle, J. A.: Modelling the potential impacts of the recent, unexpected increase in CFC-11 emissions on total column ozone recovery, Atmos. Chem. Phys., 20, 7153-7166, https://doi.org/10.5194/acp-20-7153-2020, 2020.

25 Kivi, R., Kyrö, E., Turunen, T., Harris, N. R. P., von der Gathen, P., Rex, M., Andersen, S. B., and Wohltmann, I.: Ozonesonde observations in the Arctic during 1989-2003: Ozone variability and trends in the lower stratosphere and free troposphere, J. Geophys. Res., 112, D08306, doi: 10.1029/2006JD007271, 2007.

Labitzke, K., and Naujokat, B.: The lower arctic stratosphere in winter since 1952, in SPARC Newsletter No 15, 11-14, 2000.

Langematz, U., Meul, S., Grunow, K., Romanowsky, E., Oberländer, S., Abalichin, J., and Kubin, A.: Future Arctic temperature and ozone: The role of stratospheric composition changes, J. Geophys. Res., 119, 2092-2112, doi: 10.1002/2013JD021100, 2014.

Langematz, U.: Stratospheric ozone: down and up through the Anthropocene, ChemTexts, 5 (8), 12 pp., https://doi.org/10.1007/s40828-019-0082-7, 2019.

Lee, S. H., and Butler, A. H.: The 2018-2019 Arctic stratospheric polar vortex, Weather, 75 (No. 2), 52–57, doi: 10.1002/wea.3643, 2020.

Lefèvre, F., Figarol, F., Carslaw, K. S., and Peter, T.: The 1997 Arctic ozone depletion quantified from three-dimensional model simulations, Geophys. Res. Lett., 25, 2425-2428, 1998.

Lerot C., van Roozendael, M., Spurr, R., Loyola, D. G., Coldewey-Egbers, M., Kochenova, S., van Gent, J., Koukouli, M.-E., Balis, D., Lambert, J.-C., Granville, J., and Zehner, C.: Homogenized total ozone data records from the European sensors GOME/ERS-2, SCIAMACHY/Envisat, and GOME-2/MetOp-A, Journal of Geophysical Research, 119, D07302, 2014.

Lim, E.-P., Hendon, H. H., Butler, A. H., Garreaud, R. D., Polichtchouk, I., Shepherd, T. G., Scaife, A., Comer, R., Coy, L., Newman, P. A., Thompson, D. W. J., and Nakamura, H.: The 2019 Antarctic sudden stratospheric warming, SPARC-Newsletter, 54, 10-13, 2020.

Loyola, D. G., Coldewey-Egbers, M., Dameris, M., Garny, H., Stenke, A., van Roozendael, M., Lerot, C., Balis, D., and Koukouli, M.: Global long-term monitoring of the ozone layer - a prerequisite for predictions, International Journal of Remote Sensing, 30, no. 15, 4295-4318, 2009.

Manney, G. L., Froidevaux, L., Santee, M. L., Livesey, N. J., Sabutis, J. L., and Waters, J. W.: Variability of ozone loss during Arctic winter (1991–2000) estimated from UARS Microwave Limb Sounder measurements, J. Geophys. Res.. 108, 4149, http://dx.doi.org/10.1029/2002JD002634, 2003.

Manney, G. L., Santee, M. L., Rex, M., Livesey, N. J., Pitts, M. C., Veefkind, P., Nash, E. R., Wohltmann, I., Lehmann, R., Froidevaux, L., Poole, L. R., Schoeberl, M. R., Haffner, D. P., Davies, J., Dorokhov, V., Gernandt, H., Johnson, B., Kivi, R., Kyrö, E., Larsen, N., Levelt, P. F., Makshtas, A., McElroy, C. T., Nakajima, H., Parrondo, M. C., Tarasick, D. W., von der Gathen, P., Walker, K. A., and Zinoviev, N. S.: Unprecedented Arctic ozone loss in 2011, Nature, 478 (7370), 469-475, doi: 10.1038/nature10556, 2011.

Maycock, A. C., Randel, W. J., Steiner, A. K., Karpechko, A. Y., Christy, J., Saunders, R., Thompson, D. W. J., Zou, C.-Z., Chrysanthou, A., Abraham, N. L., Akiyoshi, H., Archibald, A. T., Butchart, N., Chipperfield, M., Dameris, M., Deushi, M., Dhomse, S., Di Genova, G., Jöckel, P., Kinnison, D. E., Kirner, O., Ladstaedter, F., Michou, M., Morgenstern, O., O´Connor, F., Oman, L., Pitari, G., Plummer, D. A., Revell, L. E., Rozanov, E., Stenke, A., Visioni, D., Yamashita, Y., and

Zeng, G.: Revisiting the mystery of recent stratospheric temperature trends, Geophys. Res. Lett., 45, 9919-9933, https://doi.org/10.1029/2018GL078035, 2018.

Millán, L. F., and Manney, G. L.: An assessment of ozone mini-hole representation in reanalyses over the Northern Hemisphere, Atmos. Chem. Phys., 17, 9277-9289, https://doi.org/10.5194/acp-17-9277-2017, 2017.

5 Montzka, S. A., Dutton, R., Yu, P., Ray, E., Portmann, R. W., Daniel, J. S., Kuijpers, L., Hall, B. D., Mondeel, D., Siso, C., Nance, D. J., Rigby, M., Manning, A. J., Hu, L., Moore, F., Miller, B. R., and Elkins, J. W.: A persistent and unexpected increase in global emissions of ozone-depleting CFC-11, Nature, 557, 413-417, https://doi.org/10.1038/s41586-018-0106-2, 2018.

NCL, The NCAR Command Language (Version 6.5.0) [Software], Boulder, Colorado, UCAR/NCAR/CISL/TDD,
10 https://doi.org/10.5065/D6WD3XH5, 2018.

Newman, P. A., Nash, E. R., Rosenfield, J. E.: What controls the temperature of the Arctic stratosphere during the spring?, J. Geophys. Res., 106, 19999-20010, 2001.

Peters, D., Egger, J., and Entzian, G.: Dynamical aspects of ozone mini-hole formation, Meteorol. Atmos. Phys., 55, 205-214, https://doi.org/10.1007/BF01029827, 1995.

15 Pommereau J.-P., Goutail, F., Pazmino, A., Lefèvre, F., Chipperfield, M. P., Feng, W., van Roozendael, M., Jepsen, N., Hansen, G., Kivi, R., Bognar, K., Strong, K., Walker, K., Kuzmichev, A., Khattatov, S., and Sitnikova, V.: Recent Arctic ozone depletion: Is there an impact of climate change? Comptes Rendus Géoscience, Elsevier Masson, 350 (7), 347-353, doi: 10.1016/j.crte.2018.07.009, 2018.

Rex, M., Salawitch, R. J., von der Gathen, P., Harris, N. R. P., Chipperfield, M. P., and Naujokat, B.: Arctic ozone loss and
20 climate change, Geophys. Res. Lett., 31, L04116, doi: 10.1029/2003GL018844, 2004.

Rex, M., Salawitch, R. J., Toon, G. C., Sen, B., Margitan, J. J., Osterman, G. B., Blavier, J.-F., Gao, R. S., Donnelly, S., Keim, E., Neuman, J., Fahey, D. W., Webster, C. R., Scott, D.C., Herman, R. L., May, R. D., Moyer, E. J., Gunson, M. R., Irion, F. W., Chang, A. Y. Rinsland, C. P., and Bui, T. P.: Subsidence, mixing, and denitrification of Arctic polar vortex air measured During POLARIS, J. Geophys. Res., 104, 26611-26623, 1999.

25 Schulzweida, U.: CDO User Guide (Version 1.9.6), https://doi.org/10.5281/zenodo.2558193, 2019.

Solomon, S., Ivy, D. J., Kinnison, D., Mills, M. J., Neely III, R. R., and Schmidt, A.: Emergence of healing in the Antarctic ozone layer, Science, 353, 269-274, https://doi.org/10.1126/science.aae0061, 2016.

SPARC: SPARC Report on the Lifetimes of Stratospheric Ozone-Depleting Substances, Their Replacements, and Related Species, M. Ko, P. Newman, S. Reimann, S. Strahan (Eds.), SPARC Report No. 6, WCRP-15/2013, 2013.

Steinbrecht, W., Claude, H., Köhler, U., and Hoinka, K. P.: Correlations between tropopause height and total ozone: Implications for long- term changes, J. Geophys. Res., 103, 19183-19192, 1998.

Tilmes, S., Müller, R., Engel, A., Rex, M., and Russell III, J. M.: Chemical ozone loss in the Arctic and Antarctic stratosphere between 1992 and 2005, Geophys. Res. Lett.. 33, L20812, http://dx.doi.org/10.1029/2006GL026925, 2006.

5 Tegtmeier, S., Rex, M., Wohltmann, I., and Krüger, K.: Relative importance of dynamical and chemical contributions to Arctic wintertime ozone, Geophys. Res. Lett., 35, L17801 http://dx.doi.org/10.1029/2008GL034250, 2008.

Van Geffen, J., Van Weele, M., Allaart, M. and Van der A, R.: TEMIS UV index and UV dose operational data products, version 2. dataset, Royal Netherlands Meteorological Institute (KNMI), doi.org/10.21944/temis-uv-oper-v2, 2017.

Waibel, A. E., Peter, T., Carslaw, K. S., Oelhaf, H., Wetzel, G., Crutzen, P. J., Poeschl, U., Tsias, A., Reimer, E., and 10 Fischer, H.: Arctic ozone loss due to denitrification, Science, 283, 2064-2069, 1999.

Weber, M., Coldewey-Egbers, M., Fioletov, V. E., Frith, S. M., Wild, J. D., Burrows, J. P., Long, C. S., and Loyola, D. G.: Total ozone trends from 1979 to 2016 derived from five merged observational datasets – the emergence into ozone recovery, Atmos. Chem. Phys., 18, 2097-2117, 2018.

WMO (World Meteorological Organization), Scientific Assessment of Ozone Depletion: 1998, Global Ozone Research and 15 Monitoring Project–Report No. 44, Geneva, Switzerland, 1999.

WMO (World Meteorological Organization), Scientific Assessment of Ozone Depletion: 2002, Global Ozone Research and Monitoring Project–Report No. 47, 498 pp., Geneva, Switzerland, 2003.

WMO (World Meteorological Organization), *Scientific Assessment of Ozone Depletion: 2014*, Global Ozone Research and Monitoring Project–Report No. 55, 416 pp., Geneva, Switzerland, 2014.

20 WMO (World Meteorological Organization), Scientific Assessment of Ozone Depletion: 2018, Global Ozone Research and Monitoring Project–Report No. 58, 588 pp., Geneva, Switzerland, 2018.
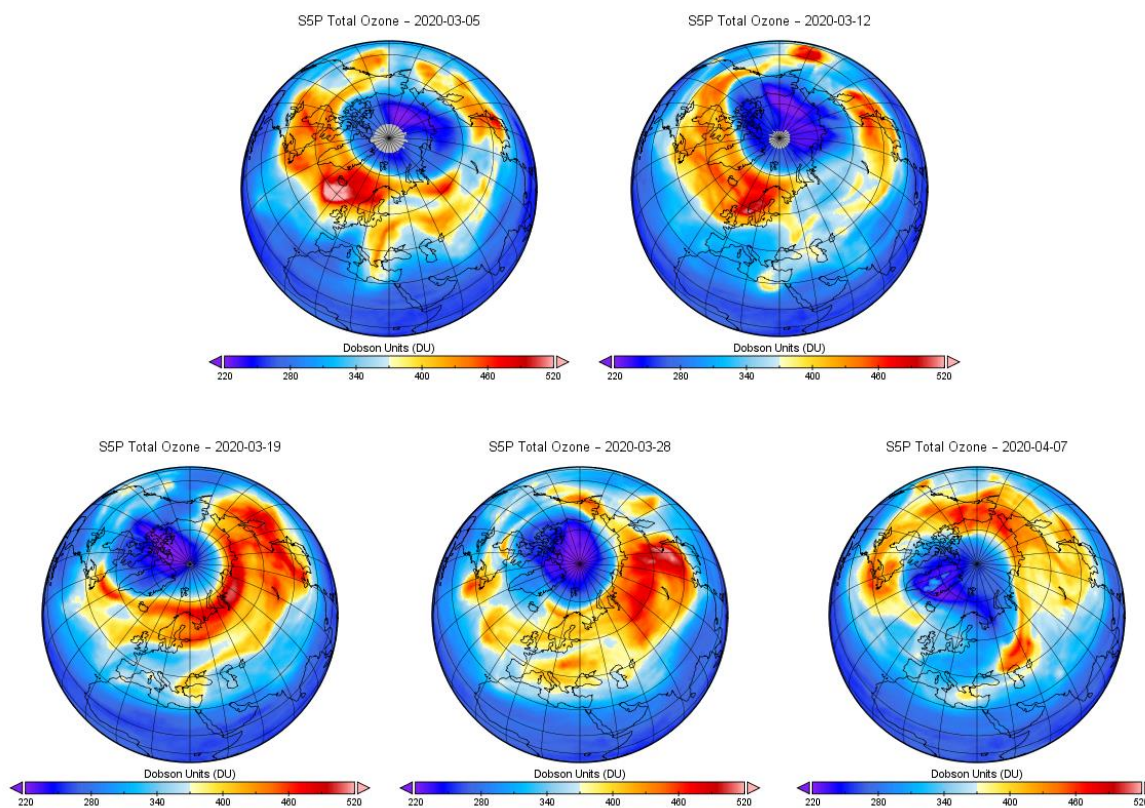
Figure 1: Total ozone column over the Northern hemisphere on March 5, 12, 19, 28 and April 7, 2020 measured by the TROPOMI instrument onboard the Sentinel-5 Precursor (S5P) satellite. Color scale is showing Dobson units (DU). The ozone hole regions with total ozone values below 220 DU are denoted with the dark purple color.
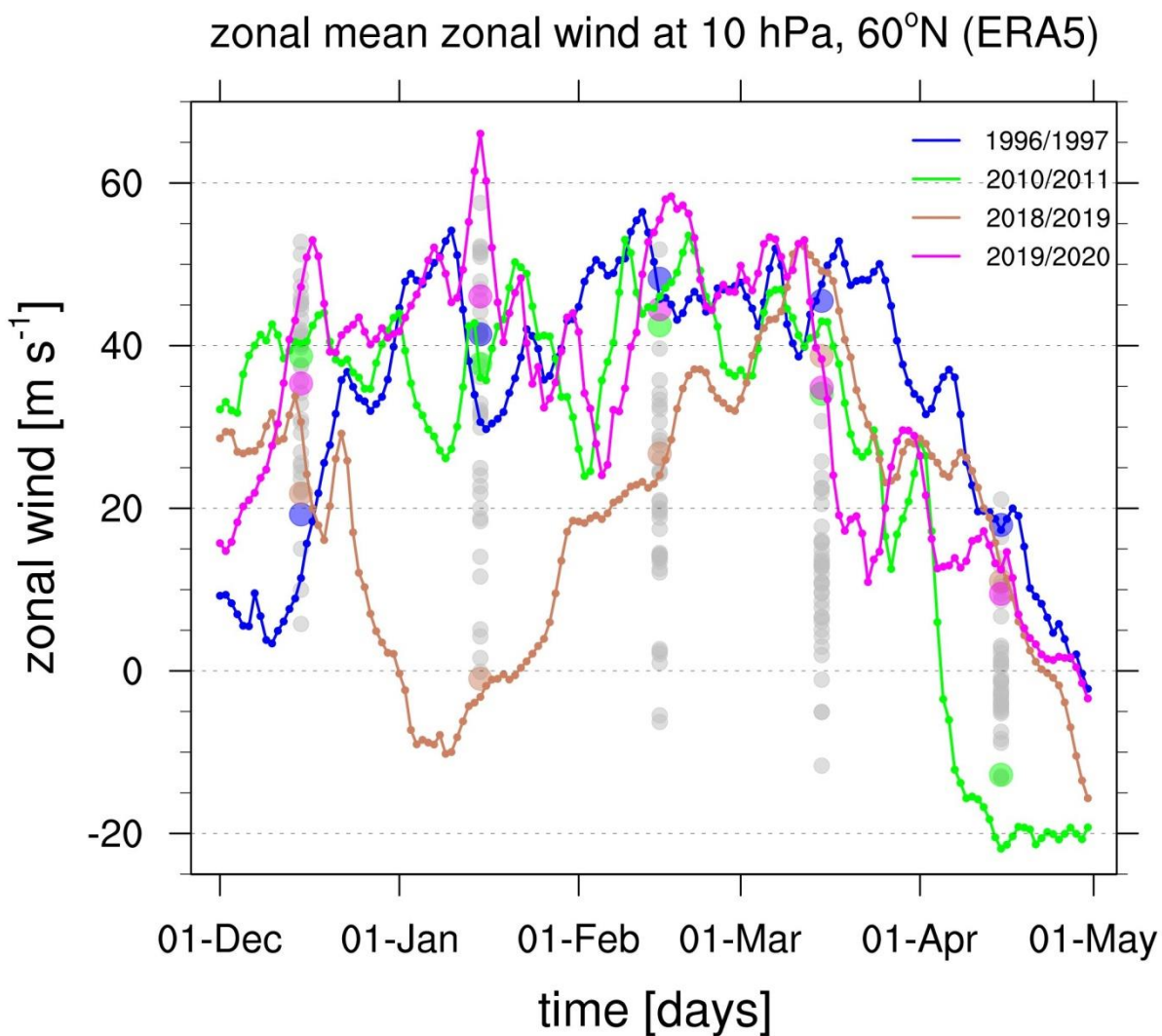
Figure 2: Daily (lines) and monthly (dots) mean zonal mean zonal wind (in m s⁻¹) at 10 hPa (about 30 km altitude) 60°N from
December 1 to April 30 based on ERA5 data. The Northern hemisphere winters 1996/1997, 2010/2011, 2018/2019 and 2019/2020
are displayed as blue, green, brown and magenta lines for daily mean and dots for monthly mean data. Additional monthly means
for the Northern hemisphere winters from 1979/1980 to 2019/2020 are shown as grey dots. For simplicity, the leap day in 2020
(February 29) was neglected in the daily time series.
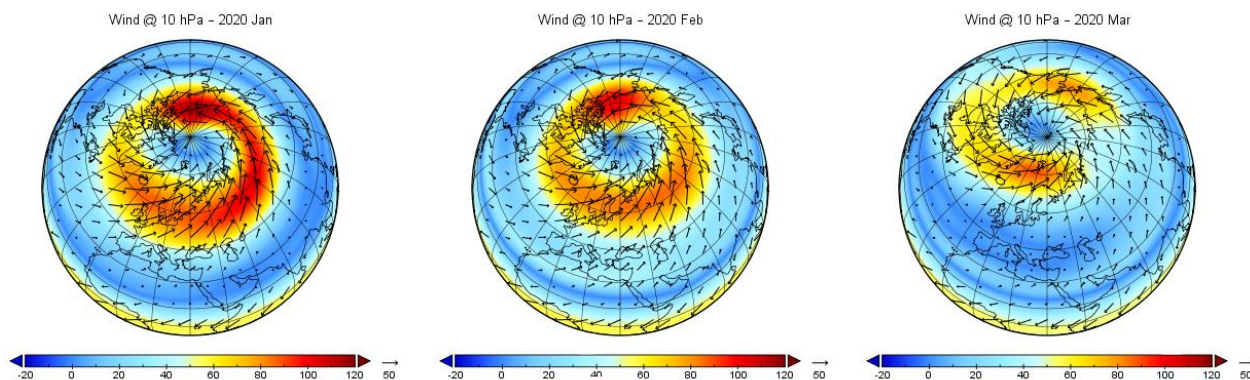
Figure 3: ERA5 monthly mean wind at 10 hPa (about 30 km altitude) showing a strong vortex in the Northern polar region with speeds of up to 118 m s^{-1}, 103 m s^{-1}, and 89 m s^{-1} for January to March 2020 respectively.
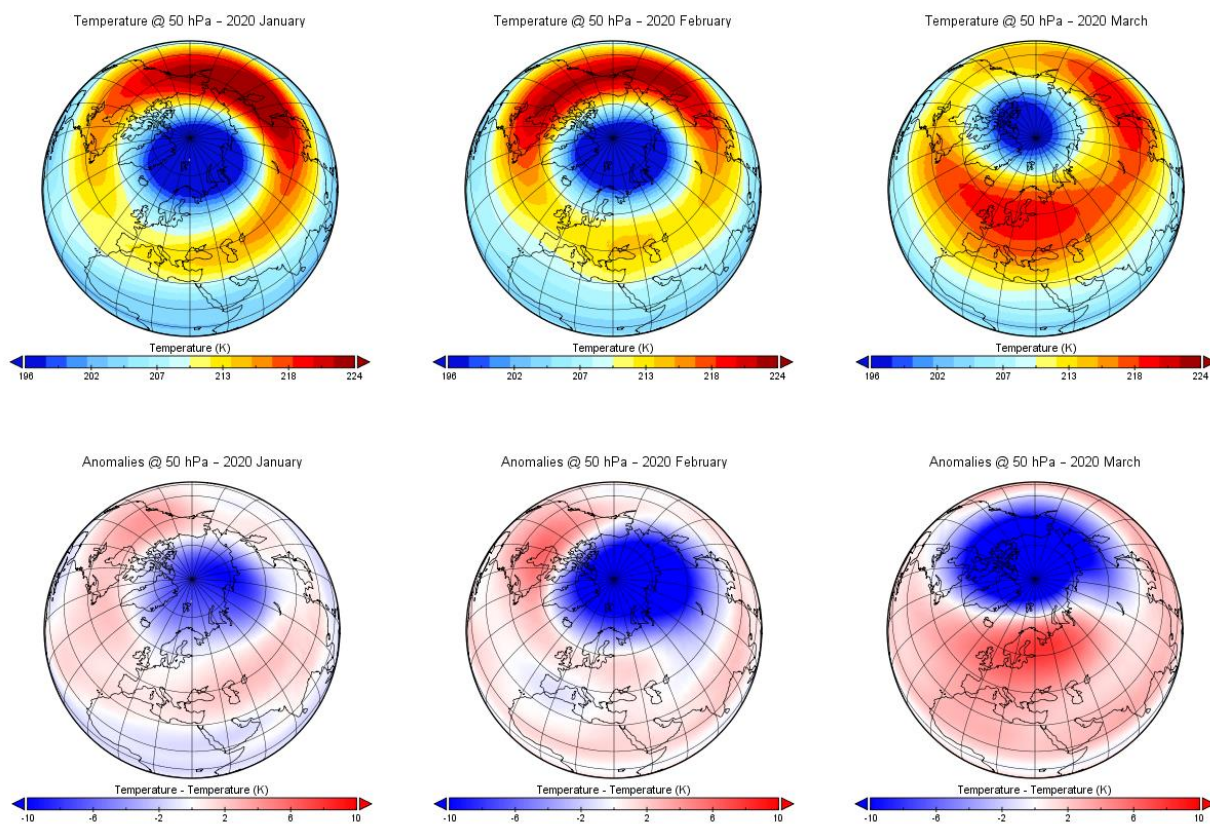
Figure 4: ERA5 monthly mean temperature at 50 hPa (about 20 km altitude) for January to March (columns 1 to 3) for year 2020 (top row) and the corresponding temperature anomalies (lower row) with respect to the average from 1979-2019 showing negative differences of up to -9.93 K in January, -18.44 K in February, and -23.83 K in March 2020.
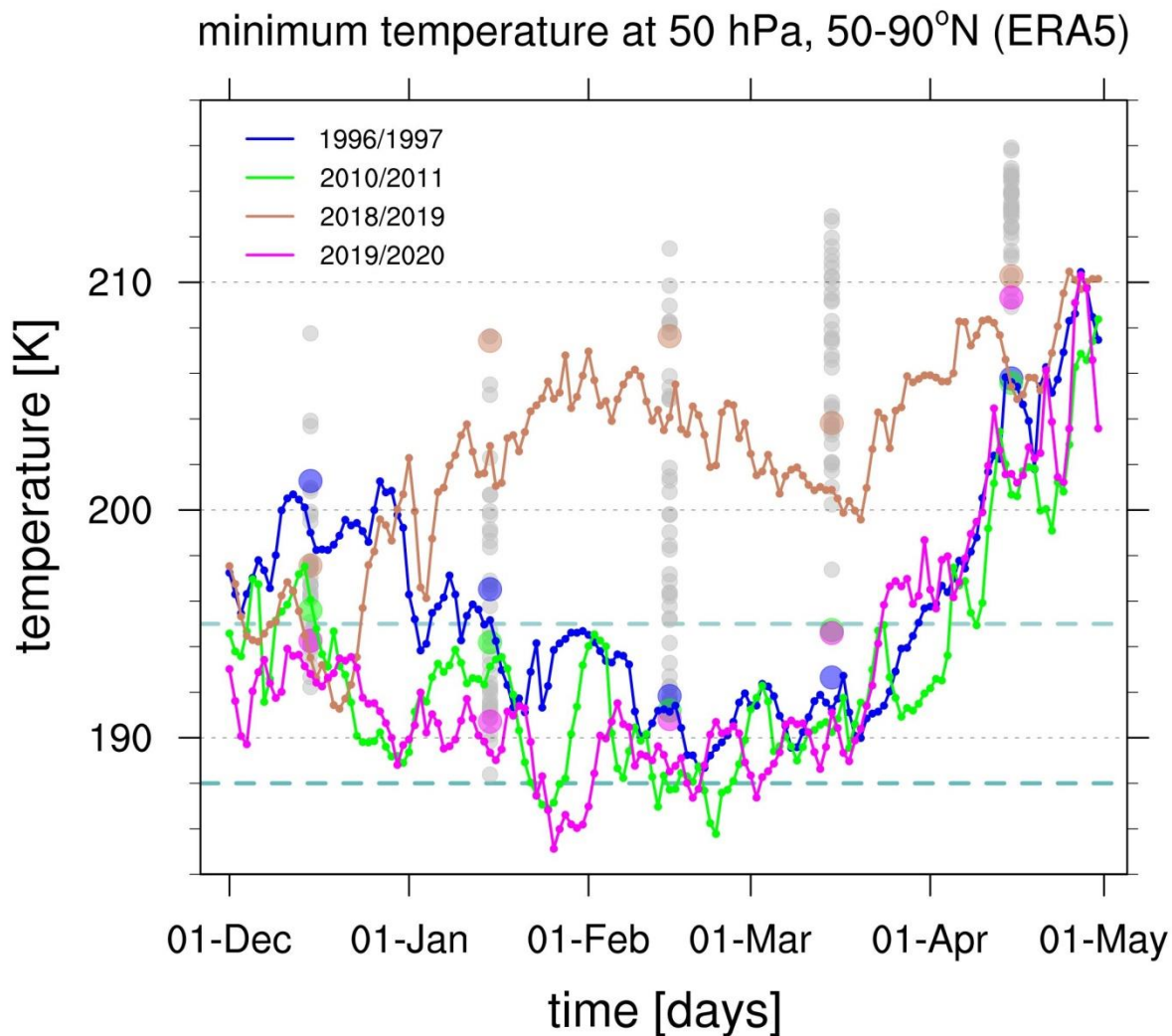
Figure 5: Minimum daily (lines) and monthly (dots) mean temperatures (in K) at 50 hPa (about 20 km altitude) for 50°N-90°N from December 1 to April 30 based on ERA5 data. The Northern hemisphere winters 1996/1997, 2010/2011, 2018/2019 and 2019/2020 are displayed as blue, green, brown and magenta lines for daily mean and dots for monthly mean data. Additionally, the minima of the monthly mean temperature data for the Northern hemisphere winters from 1979/1980 to 2019/2020 are shown as grey dots. For simplicity, the leap day in 2020 (February 29) was neglected in the daily time series. The dark green broken horizontal lines at 195 K and 188 K marked the thresholds for the formation of NAT-PSC and ICE-PSC, respectively (see text).
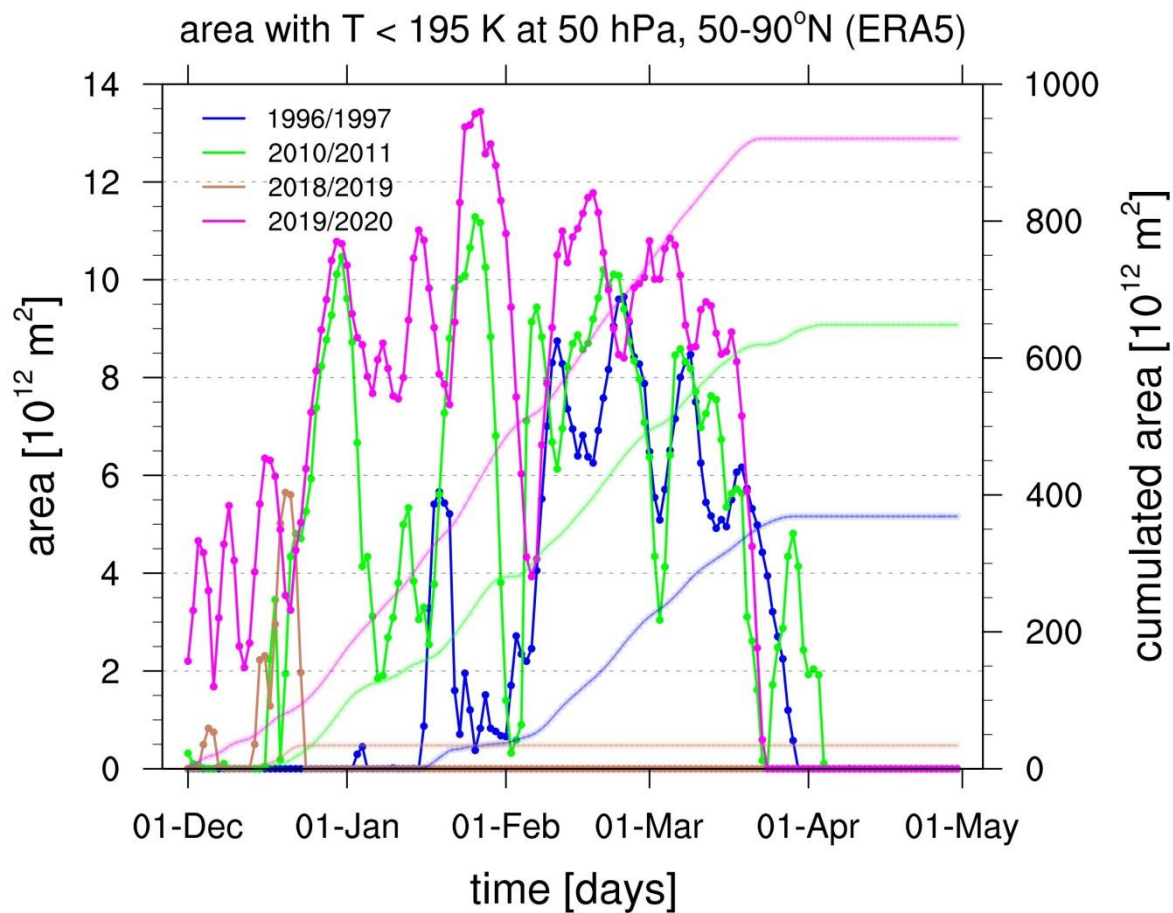
Figure 6: Daily area (in 10¹² m²) with temperature less than 195 K at 50 hPa (about 20 km altitude) in the region 50°N-90°N from December 1 to April 30 based on ERA5 data (solid lines). Daily cumulated values are indicated as faint lines. The Northern hemisphere winters 1996/1997, 2010/2011, 2018/2019 and 2019/2020 are displayed as blue, green, brown and magenta lines, respectively. For simplicity, the leap day in 2020 (February 29) was neglected in the daily time series.
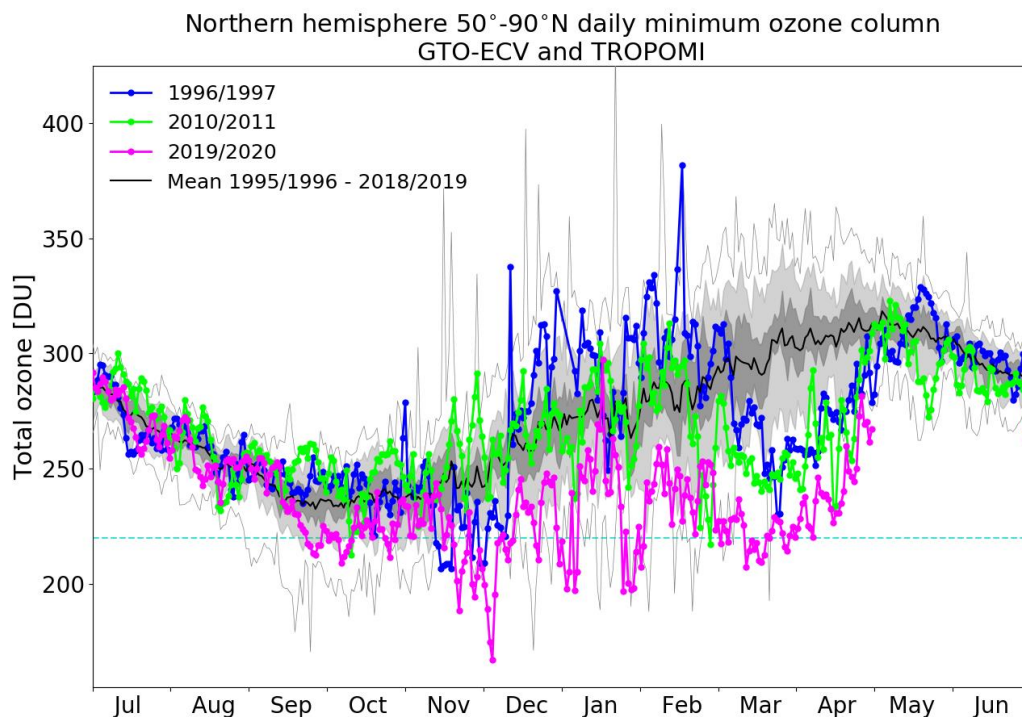
Figure 7: Annual cycle of the minimum total column ozone values (in Dobson Units, DU) in the Northern polar region between 50°N and 90°N derived from the European satellite data record GOME-type Total Ozone Essential Climate Variable (GTO-ECV) from July 1995 to June 2019 and TROPOMI data from July 2019 to April 2020. The thick black line shows the GTO-ECV mean
5   **annual cycle with lowest ozone values in fall season (October, November) and highest ozone values in late spring (April, May). The thin black lines indicate the maximum and minimum values for the complete time period of satellite measurements starting in 1995. The light grey shading denotes the 10th percentile and the 90th percentile, and the dark grey shading denotes the 30th percentile and the 70th percentile, respectively. The magenta line shows the minimum values for the TROPOMI total ozone in the 2019/2020 cycle. The blue and green lines show the minimum values for the total ozone in the years 1996/1997 and 2010/2011,**
10   **respectively. Note the conspicuous phase of persistent low ozone values below 220 DU (dashed cyan line) in March and April 2020 with new record values for this time of the year.**
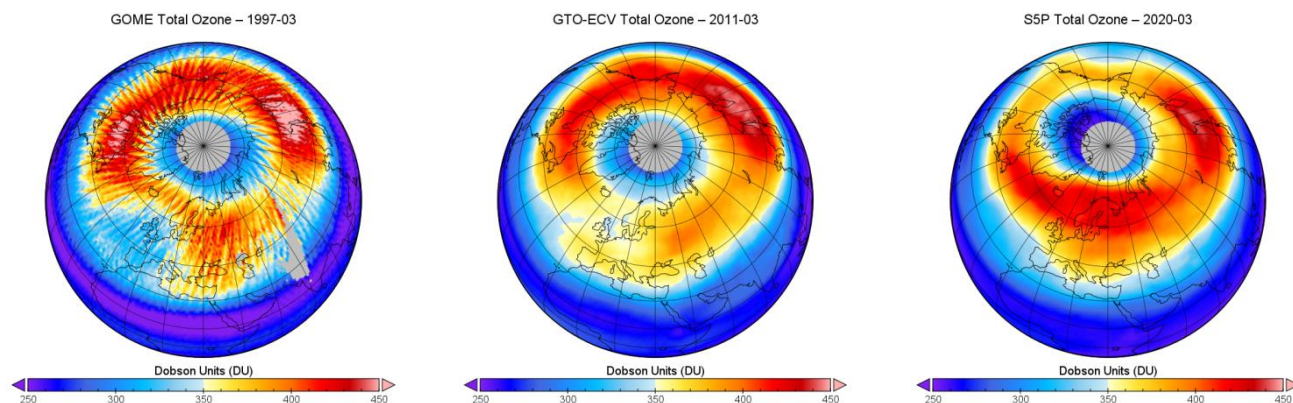
Figure 8: Monthly mean total ozone columns over the Northern hemisphere in March 1997 (left), March 2011 (middle), and March 2020 (right). The plot for March 1997 is based on GOME/ERS-2 data with a limited spatial sampling, which induces the orbit structures on the monthly mean values.